EFFECT OF UNBALANCE ON A JOURNAL BEARING UNDERGOING OIL WHIRL

L. E. BARRETT, BS, MS
University of Virginia, Charlottesville, Virginia, U.S.A.
A. AKERS, BSc, MSc, PhD, CEng, FRAeS, MASME
Iowa State University of Science and Technology, Engineering Research Institute, Ames, Iowa, U.S.A.
E. J. GUNTER, BS, MS, PhD, MASME
University of Virginia, Charlottesville, Virginia, U.S.A.

SYNOPSIS A time-transient nonlinear analysis has been developed to examine the dynamical limit cycle motion of a plain journal bearing. The effect of unbalance and ambient pressure on the journal limit cycle motion below and above the linearized stability threshold speed is examined.

The short bearing approximation is used, and the assumption of a 180° oil film has been relaxed. An arbitrary film extent based upon the instantaneous values of journal displacement, velocity, and ambient pressure is used.

It has been found possible to optimize the unbalance to minimize the amplitude and the force transmitted for limit cycle operation above the stability threshold speed. Below this optimum value the whirl is fractional frequency and above this value it is synchronous.

It has been found that when the journal is operating above the stability threshold speed, rotor unbalance may result in a smaller limit cycle than the balanced rotor. The effect of a non-zero ambient pressure at the optimum value of unbalance is to increase the size of the limit cycle and make the motion nonsynchronous.

1. INTRODUCTION

Although it has been recognized that the balanced journal bearing exhibits instability above a certain operating speed (1, 2)*, little research has been conducted showing the effects of unbalance and ambient pressurization on the size of the nonlinear limit cycle motion.

In all rotating machinery some level of unbalance usually exists. If the journal is operating above the stability threshold speed, the effect of unbalance is to impress a synchronous component of whirl onto the half frequency whirl motion of the unstable, balanced rotor. If the unbalance exceeds a certain level, the half frequency component of the rotor motion is entirely suppressed resulting in purely synchronous motion. The unbalance level required for this phenomenon to occur depends on the speed of the rotor above the stability threshold speed and the ambient pressure level. It is thus possible to introduce nonsynchronous whirl motion attended by larger orbiting of the journal and higher forces transmitted to the rotor support structure by refining the balance of a rotor operating above the stability threshold speed and by increasing the ambient pressure level.

By applying general ambient pressure to the ends of the bearing such that the cavitation pressure is below ambient, the extent of the cavitated film region is altered significantly. This results in a decrease in the stability threshold speed. It is also necessary in this case to increase the amount of unbalance required to suppress nonsynchronous whirl when operating above the threshold speed.

In order to perform the analysis, the short bearing approximation was applied to the Reynolds equation with an accompanying modification to the axial boundary conditions. This allows the formation of cavitated regions of arbitrary extent. To facilitate the incorporation of the hydrodynamic forces with the journal equations of motion, the Reynolds equation was written in cartesian rather than polar coordinates. The integration of the resulting pressure distribution was performed numerically using Weddle's rule, and the equations of motion were integrated numerically using a modified Euler Method. The resulting time-transient orbits were automatically plotted by the computer.

* References are given in the Appendix.

2. NOTATION

c	radial bearing clearance
e_u	journal mass unbalance eccentricity
EMU	unbalance eccentricity ratio = e_u/c
F	total bearing fluid film force = $\sqrt{F_x^2 + F_y^2}$
F_x	bearing fluid film force in x-direction
F_y	bearing fluid film force in y-direction
$\bar{F}_x$	$F_x/(mc\omega^2)$
$\bar{F}_y$	$F_y(mc\omega^2)$
FU	unbalance force = $me_u\omega^2$
h	bearing fluid film thickness
L	bearing length
m	journal mass
N'	journal speed, rev/sec

p total bearing fluid film pressure

p_a ambient pressure

P_m maximum bearing hydrodynamic pressure

R bearing radius

S Sommerfeld number $= \frac{\mu N' LD}{W}\left(\frac{R}{c}\right)^2$

t time

T ωt

TRD dynamic force transmissibility coefficient $= F/me_u\omega^2$

W journal weight

W_{xext} external load applied to journal in x-direction

W_{yext} external load applied to journal in y-direction

$\bar{W}_{xext}$ $W_{xext}/mc\omega^2$

$\bar{W}_{yext}$ $W_{yext}/mc\omega^2$

x journal displacement in x-direction

$\dot{x}$ journal velocity in x-direction (dx/dt)

$\ddot{x}$ journal acceleration in x-direction (d^2x/dt^2)

X x/c

X' dX/dT

X'' d^2X/dT^2

y journal displacement in y-direction

$\dot{y}$ journal velocity in y-direction (dy/dt)

$\ddot{y}$ journal acceleration in y-direction (d^2y/dt^2)

Y y/c

Y' dY/dT

Y'' d^2Y/dT^2

z axial coordinate

Z $2z/L$

ε eccentricity ratio, e/c

θ circumferential coordinate

μ lubricant viscosity

ϕ journal attitude angle

ψ journal unbalance displacement phase angle

ω journal angular velocity

3. THEORY

The Reynolds equation for a short journal bearing in fixed cartesian coordinates is given (3, 4) as

$$\frac{\partial}{\partial z}\left[\frac{h^3}{6\mu}\frac{\partial p}{\partial z}\right] = \omega\frac{\partial h}{\partial \theta} + 2\frac{\partial h}{\partial t} \tag{1}$$

For the cylindrical bearing the film thickness is

$$h = c - x\cos\theta - y\sin\theta$$

If the viscosity is assumed constant and journal is not misaligned axially, equation (1) may be integrated twice to give the pressure distribution in the bearing. The boundary conditions are that the ambient pressure at each end of the bearing is p_a. Thus

$$p(\theta, z) = \frac{3}{4}\frac{\mu L^2}{h^3}\left[\omega\frac{\partial h}{\partial \theta} + 2\frac{\partial h}{\partial t}\right] \times \left[\left(\frac{2z}{L}\right)^2 - 1\right] + p_a \tag{2}$$

letting

$$P_m = -\frac{3}{4}\frac{\mu L^2}{h^3}\left[\omega\frac{\partial h}{\partial \theta} + 2\frac{\partial h}{\partial t}\right]$$

the pressure distribution becomes

$$p(\theta, z) = P_m\left[1 - Z^2\right] + p_a \tag{3}$$

The fluid film is assumed to cavitate whenever $p < 0$. For a given circumferential position the axial location, Z_c, where the pressure is zero is given by

$$Z_c = \sqrt{1 + \frac{p_a}{P_m}}$$

This expression is valid whenever $P_m < 0$ and $|P_m| > p_a$.

Subject to these cavitation conditions, the force components on the journal due to the fluid film pressure are found by integrating the pressure over the journal surface. Thus the force components are

$$F_x = -L\int_0^{2\pi}\int_{Z_c}^{1} p(\theta, Z)\cos\theta\, R\, dZ\, d\theta \tag{4}$$

$$F_y = -L\int_0^{2\pi}\int_{Z_c}^{1} p(\theta, Z)\sin\theta\, R\, dZ\, d\theta \tag{5}$$

When the integration in the z-direction is performed in closed form, the forces become

$$F_x = -RL\int_0^{2\pi}\left\{P_m(\theta)\left[\frac{Z_c(\theta)^3}{3} - Z_c(\theta) + \frac{2}{3}\right]\right.$$

$$+ \; p_a \left[1 - Z_c\right]\Bigg\} \cos\theta \, d\theta \qquad (6)$$

$$F_y = - RL \int_0^{2\pi} \Bigg\{ P_m(\theta) \left[\frac{Z_c(\theta)^3}{3} - Z_c(\theta) + \frac{2}{3}\right] + p_a \left[1 - Z_c\right]\Bigg\} \sin\theta \, d\theta \qquad (7)$$

Equations (6) and (7) are integrated numerically to give the resulting forces. The integration in the axial direction has been performed analytically to simplify the numerical calculations. It is convenient to non-dimensionalize the journal displacement and velocity as follows.

$$X = \frac{x}{c}, \qquad Y = \frac{y}{c}, \qquad T = \omega t,$$

$$X' = \frac{\dot{x}}{c\omega}, \qquad Y' = \frac{\dot{y}}{c\omega}$$

where the prime denotes differentiation with respect to T. Subject to this non-dimensionalization, the expression for the centreline bearing hydrodynamic pressure becomes

$$P_m(\theta) = - \frac{3}{4} \frac{\mu L^2 \omega}{c^2} \; X \left[\frac{X\sin\theta - Y\cos\theta - 2(X'\cos\theta + Y'\sin\theta)}{(1 - X\cos\theta - Y\sin\theta)^3}\right] \qquad (8)$$

The dynamical motion of the journal assumes that the journal is a point mass without gyroscopic effects. The journal is also assumed to rotate at constant angular velocity and to be unbalanced with the journal mass displaced at a distance e_u from the journal geometric centre. The equations of motion are

$$\ddot{mx} = me_u\omega^2\cos\omega t + F_x + W_{xext}(t) \qquad (9)$$

$$\ddot{my} = me_u\omega^2\sin\omega t + F_y + W_{yext}(t) - W \qquad (10)$$

and in dimensionless form,

$$X'' = EMU\cos T + \bar{F}_x + \bar{W}_{xext}(T) \qquad (11)$$

$$Y'' = EMU\sin T + \bar{F}_y + \bar{W}_{yext}(T) - \bar{W} \qquad (12)$$

These equations were programmed to be integrated numerically to calculate the transient motion of the journal under arbitrary unbalance and steady or time dependent load conditions.

4. JOURNAL NONLINEAR TRANSIENT MOTION: DESCRIPTION OF THE TRANSIENT PROGRAMME

The transient nonlinear journal bearing programme as described in (4, 5) allows one to start the shaft motion at any given position with arbitrary initial velocity. The origin of the X-Y coordinate system is taken as the bearing centre as shown in Fig. 1, and the circle of unity radius drawn about the origin of the coordinate system as shown in Fig. 2 represents the bearing clearance circle. The shaft centre therefore is constrained to remain within the bearing clearance circle. If the dimensionless shaft eccentricity equals or exceeds unity, then physical contact between the shaft and bearing is assumed to have occurred.

The use of the fixed X-Y coordinate system was chosen following the procedure developed by Castelli (3) who first used a fixed cartesian coordinate system for the analysis of the stability and transient motion of the 360° journal bearing with a compressible lubricant. The fixed cartesian coordinate system has several important advantages over the normal polar coordinate representation which has been used extensively in the past in bearing analysis. The major advantage of the polar coordinate system is the ease by which analytic expressions for the bearing force terms may be obtained for the 360° and the 180° film cases. If the film extent is neither π or 2π radians, then even for the polar coordinate system, the film force expressions are difficult to obtain for general cavitation conditions. An extensive analytic treatment of the short bearing forces in polar coordinates is given by Lund (6) and Holmes (7) for the 180° film. There are five major reasons for the use of the fixed cartesian coordinate representation for bearing motion. These are:

(1) The kinematic expressions for the journal motion are linear.

(2) The bearing forces are easily obtainable by numerical integration of the cavitated pressure film.

(3) The bearing linear stiffness and damping coefficients are readily obtainable by numerical perturbations about the equilibrium position.

(4) The dynamical system may be readily extended to more complex multi-mass, multi-bearing flexible rotor systems (8).

(5) The procedure is adaptable to noncircular bearing geometries (9).

The journal motion is determined numerically by means of a standard time integration procedure. It has been found sufficient to use from 100 to 200 steps per cycle of shaft motion, and up to 10 cycles of motion may be obtained in one run.

On the computer plots of the journal motion, a small timing mark circle is placed on the orbit after each cycle of shaft motion. In addition to the calculation of the journal motion, the instantaneous bearing force and whirl ratio are computed and recorded. The position at which the maximum hydrodynamic force occurs is indicated by an asterisk. It is possible to obtain also the maximum hydrodynamic fluid film pressure generated in the bearing during the motion. The knowledge of this maximum pressure is of value as it affects the extent of the cavitation region in the bearing for the ambient pressure chosen.

5. ROTOR MOTION BELOW STABILITY THRESHOLD SPEED

In order to check whether the programme was working satisfactorily, recourse to previous work was made. The journal was given conditions shown in (10), and a transient analysis was conducted. The transient using zero unbalance is shown in Fig. 2, and it is seen that the value of a steady state eccentricity and attitude angle are as calculated from theory.

($\varepsilon_o = 0.7$, $\phi_o = 38.7°$). Fig. 2 represents a typical computer plot of the motion of a balanced horizontal journal. The system represents a 178 N (40 lb) rotor of journal length L = 21 mm (0.825 in) with a shaft diameter of D = 63.5 mm (2.50 in), a bearing radial clearance of c = 0.1524 mm (0.006 in), and a shaft speed of 2,416 rev/min. The Sommerfeld number is 0.303 in this case and the ambient pressure p_a is taken to be zero. Therefore, the film is assumed to cavitate whenever the pressure $P_m(\theta) < 0$. The journal motion is initiated at the origin with zero velocity. The journal drops down almost vertically due to the gravitational loading to an eccentricity ratio of approximately 0.6. The maximum film force recorded is 327 N (73.5 lb) which occurs at an eccentricity ratio Of 0.55. When the shaft is released, the radial squeeze film forces are a maximum when the shaft centre has its highest velocity which occurs at an eccentricity ratio of about 0.3. As the vertical shaft velocity decreases and the "wedge effect" forces predominate, in this case above eccentricity ratios of 0.5, the shaft centre moves rapidly in the horizontal direction and spirals inward to its stable equilibrium position. If a high ambient pressure were assumed such that cavitation is not possible, then the system is inherently unstable, and the shaft motion orbits outward in half frequency whirl motion similar to that shown in Fig. 5.

Fig. 3 represents the steady state synchronous orbits obtained from various values of unbalance varying from EMU = 0.1 to 1.0 for the system corresponding to Fig. 2 operating below the stability threshold speed. The orbits depicted here are similar to the ones shown by Holmes in reference (11). The orbits obtained for the low unbalance eccentricities of EMU = 0.1 and 0.2 are nearly elliptical in shape. These trajectories and the resulting forces transmitted can be closely approximated by linear theory.

As the unbalance eccentricity becomes larger, for instance when EMU = 0.5 and 0.6, the orbits depart from the elliptic shape, and the centre of the orbit is not the steady-state balanced equilibrium position as it is for the lower values of EMU. When the unbalance is increased to EMU = 0.8, the orbit crosses the horizontal axis. It is of interest to note that the orbit in the lower right quadrant of the bearing ($\frac{3\pi}{2} \leq \theta \leq 2\pi$) is almost a circular arc. There is little change in this part of the trajectory for increasing unbalance levels.

When the rotating load approaches the static load or weight of the journal as in the case when EMU = 1.0, then the orbit will enclose the bearing centre. In this case perturbated bearing theory cannot be used to accurately calculate the rotor orbit and the transmitted bearing forces. If the journal unbalance is increased such that EMU > 1.0 so that the rotating load is substantially higher than the journal static load, the orbit will be almost circular in nature with its centre at the bearing centre. In this case the analytic bearing nonlinear radial and tangential forces may be used to calculate the circular synchronous unbalance orbit. It has been observed that in all cases where the unbalance eccentricity EMU is equal to or exceeds unity, the dynamic transmissibility will also be greater than one. This implies that the force transmitted to the bearing housing will be larger than the rotating unbalance force.

Fig. 4a represents the transient motion of a heavily loaded balanced journal released from the bearing centre. In this case, the shaft drops almost vertically until it reaches an eccentricity ratio of 0.85 before it moves horizontally to reach its equilibrium position $\varepsilon_o = 0.81$ and $\phi = 25°$. Due to the high eccentricity and zero ambient pressure of the system in Fig. 4, the journal is highly stable and self excited whirl cannot be initiated at this speed. The maximum force occurs at the point corresponding to the asterisk and is 180 N (40.5 lb) above the static loading of 36 N (8 lb).

The initial starting point of the trajectory in Fig. 4b was taken as $\varepsilon(0) = 0.8$ and $\phi(0) = 90°$. The resulting trajectory is identical to the orbit shown by Capriz in Fig. 16 of his comments to the Holmes paper (2). In his analysis, Capriz considers cavitation and assumes a π sector film. The maximum force transmitted in Fig. 4b with the diffierent starting conditions was 88 N (19.7 lb) due to the higher shaft velocity and corresponding higher squeeze film forces. The final steady state equilibrium position is the same regardless of the starting position.

In Fig. 5 the bearing is identical to the system shown in Fig. 4 except that the ambient pressure has been increased to 3.41 MPa (500 lb/in^2). The high increase in the bearing ambient pressure reduces the extent of cavitation. When the journal is released, the motion is no longer a damped stable trajectory which rapidly reaches its equilibrium position, but spirals outward with fractional frequency whirl. It is significant that the journal forms a limit cycle and the motion does not continue to increase with time nor does the journal ever contact the bearing surface. Only if cavitation is entirely prevented will the journal contact the bearing surface.

6. ROTOR MOTION ABOVE STABILITY THRESHOLD SPEED

6.1. Effect of Unbalance

Fig. 6 shows a typical transient orbit of a lightly loaded journal with low unbalance running above the stability threshold speed. Mitchell, Holmes, and Byrne (2), Badgley (1), Kirk (4), and others have demonstrated that the stability threshold speed for zero ambient pressure (180° film bearing) for steady state eccentricity ratios below 0.7 is

$$\omega_s = 2.5 = \omega\sqrt{\frac{mc}{W}} \tag{13}$$

The appropriate stability threshold then for the lightly loaded, balanced, horizontal rotor in rev/min is given by

$$N_s = 24\sqrt{\frac{g}{c}} \tag{14}$$

For the 0.127 mm (0.005 in) clearance in Fig. 6, the stability threshold speed is approximately N_s = 6,668 rev/min. It is therefore apparent that the journal is operating well over 50% above the threshold speed. In Fig. 6, the journal was started at the bearing centre with zero initial velocity. The small rotating unbalance load on the journal causes the journal to attempt to orbit outward with synchronous precession. After a half cycle of shaft motion, the fluid film bearing forces predominate over the rotating unbalance force causing the orbit to be essentially circular with half-frequency whirl about the bearing centre. It can be seen that the journal does not contact the bearing surface even though the system is operating well above the stability threshold speed.

Numerous authors (1, 2, 3) have examined the fractional frequency whirl motion of a journal

operating above the stability threshold speed. In a number of these investigations it has been shown that the journal will orbit outward until it contacts the bearing surface although no such behavior has been observed experimentally. Shawki (12) reported in his studies of the lightly loaded journal that bearing contact was never obtained and that the maximum whirl eccentricity did not exceed 0.81.

The bearing radial and tangential force equations for the uncavitated short bearing are given by

$$F_r = -\frac{RL^3}{c^2}\mu\frac{\pi\dot{\varepsilon}(1+2\varepsilon^2)}{(1-\varepsilon^2)^{5/2}} \quad (15)$$

$$F_\phi = \frac{RL}{2c}\mu\pi\frac{(\omega-2\dot{\phi})\varepsilon}{(1-\varepsilon^2)^{3/2}} \quad (16)$$

Such a system has been shown to be completely unstable with half frequency whirl at all speeds by Robertson (13) over 40 years ago, and he stated that the whirl orbit would grow until it equaled the bearing clearance. Poritsky (14) later demonstrated that a hydrodynamic bearing can have a finite stability threshold only if it develops a radial restoring spring force. For the uncavitated bearing the radial restoring force of equation (15) is a function of journal velocity and not shaft rotation or precession. Hence in this case the radial restoring force is entirely damping in nature and has no restoring spring characteristic as specified by Poritsky for stability. Thus in this system the journal will continue to orbit outward until contact with the bearing surface occurs. Such whirl orbits have been demonstrated analytically by Reddi (15), Holmes (16), and others. It is now well recognized that film cavitation plays an essential role in the stability threshold of a bearing.

Fig. 7 represents a bearing similar to Fig. 6 except that the rotor unbalance has been increased from EMU = 0.08 to 0.2. This creates a rotating unbalance load FU = 698 N (157 lb) acting on the journal. The rotor motion is started at the bearing centre with zero initial velocity. The shaft motion spirals outward with a combination of synchronous and half frequency whirl. The combination of these two vectors produces the characteristic internal loop associated with oil film whirl with an unbalanced journal (17). Note that the limit cycle with unbalance of EMU = 0.2 in Fig. 7 is significantly smaller than the limit cycle obtained for the balanced rotor shown by the dashed line.

In Fig. 6 the rotating load was 278 N (62.6 lb) and the maximum force transmitted was 950 N (213.5 lb) which represents an equivalent dynamic transmissibility of TRD = 3.41. In Fig. 7 with the unbalance load increased to 698 N (157 lb) the maximum force transmitted is reduced to 943 N (212 lb) which represents a dynamic transmissibility of 1.35. Therefore due to the bearing nonlinear characteristics, an increase in rotor unbalance can actually result in smaller amplitudes of motion and forces transmitted when operating above the stability threshold speed.

Fig. 8 shows the results of further increases in unbalance eccentricity. When EMU is increased to 0.22, the synchronous component of the whirl motion becomes larger as indicated by the increase in size of the inner loop. Although only a slight reduction in the overall orbit size has occurred, the dynamic transmissibility ratio has decreased from 1.35 to 1.25. For this case the rotating unbalance load is 765 N (172 lb), and the transmitted force is 952 N (214 lb). Increasing the rotating load to 876 N (197 lb), EMU = 0.25, results in a smaller nonsynchronous whirl component and a reduction in the orbit size. The transmissibility has been significantly reduced to TRD = 1.03 indicating that the transmitted force is 898.5 N (202 lb). Another increase of rotating load to 903 N (203 lb), EMU = 0.26 has resulted in a completely synchronous circular limit cycle. The centre of the orbit is displaced from the bearing centre. Therefore, the addition of rotor unbalance to a system operating above the stability threshold speed for static loading will eliminate the instability and a suitable rotating load can always be found to produce synchronous whirl for a given ambient pressure level.

There appears to be an optimum unbalance to incorporate in the rotor system when operating above the stability threshold speed to produce the minimum amplitude of motion and dynamic transmissibility. Fig. 9 represents the dynamic transmissibility and the unbalance displacement phase angle ψ vs unbalance eccentricity for the two speeds of 10,500 and 15,500 rev/min which are well above the stable speed range of operating for the balanced rotor. Fig. 9a shows that as the unbalance is increased for both speeds, the dynamic transmissibility reduces to a minimum value. This minimum value represents the transition point where the half frequency whirl motion is completely suppressed and only synchronous motion remains. The optimum value of unbalance to suppress the whirl motion for the 10,500 rev/min case is EMU = 0.26. For the 15,000 rev/min case, the required unbalance eccentricity ratio to produce stable operation increases to EMU = 0.31. In general, the higher the speed above the stability threshold speed, the higher will be the value of unbalance required to produce stable operation. This result cannot be obtained from the linearized bearing stiffness and damping coefficients calculated by perturbations about the equilibrium position.

Table 1 lists the maximum limit cycle amplitudes and transmitted forces for various values of unbalance for the rotor of Fig. 9 for the 10,500 rev/min case. As the unbalance increases to a value of EMU = 0.26, the limit cycle reduces from 0.75 to 0.29. The table shows when the unbalance increases beyond this value, the synchronous limit cycle increases in amplitude as does the dynamic transmissibility as shown also by Fig. 9. Although the introduction of unbalance will produce stable motion and a reduction of the whirl amplitude above that experienced with the balanced rotor configuration when operating above the stability threshold speed, this procedure is not necessarily recommended as good design practice because of the large bearing forces transmitted. This is particularly pronounced when operating at very high speeds.

6.2. Effect of Ambient Pressure

The effect of increase of ambient pressure is to increase the size of the limit cycle at the optimum value of EMU (0.26). Fig. 10 shows how the limit cycle is increased as ambient pressure is increased. A further important point is that the motion is now transformed from synchronous into fractional frequency whirl behavior. This was observed to occur for ambient pressures as low as 0.034 MPa (5.0 lb/in^2). No bearing contact was encountered with increasing ambient pressure. Only if the ambient pressure were considered infinite

such that cavitation did not practically occur would the journal motion grow until it completely filled the bearing clearance.

7. CONCLUSIONS

(1) The representation of the hydrodynamic bearing pressure in fixed cartesian rather than polar coordinates provides for simpler transient journal analysis in which the ambient pressure effects may be readily incorporated.

(2) Journal steady state equilibrium positions and steady state orbits as determined by the transient method are independent of the initial position of the journal as is the nonlinear limit cycle motion obtained above the stability threshold speed.

(3) If cavitation occurs, the journal does not contact the bearing surface when operated above the stability threshold speed. A limit cycle is instead formed, the size being determined by the extent of the cavitated region in the film. These limit cycle orbits are due to the nonlinearity of the hydrodynamic forces and cannot be determined from linearized bearing characteristics.

(4) Increasing the ambient pressure above the fluid cavitation pressure reduces the extent of the cavitated region resulting in a reduction in the journal stability threshold speed and an increase in the size of the limit cycle when operating above the stability threshold speed.

(5) The application of unbalance to a journal operating above the stability threshold speed introduces a synchronous component to the half frequency unstable whirl motion. Increasing unbalance magnitudes reduces the half frequency component of the whirl motion.

(6) If cavitation occurs, it is possible to optimize the unbalance level such that the amplitude of the limit cycle and dynamic force transmissibility are minimized. This optimum value of unbalance results in complete suppression of half frequency whirl.

(7) Although the intentional introduction of unbalance into a rotor system to suppress non-synchronous whirl is not recommended, this study shows how the inherent instability of a journal may be masked by rotor unbalance. Refinement of the state of balance of the rotor may actually lead to larger amplitude, unstable whirl orbits of the rotor. This has been observed by authors in rotor-bearing experimental rigs.

8. ACKNOWLEDGEMENTS

The authors wish to express their appreciation to William J. Anderson, Chief, Bearings Branch, and Robert E. Cunningham, Project Manager, NASA Grant NGR-47-005-050, NASA Lewis Research Center, for support of this research. Appreciation is also given to the Department of Mechanical Engineering, School of Engineering and Applied Science, University of Virginia for computer support.

APPENDIX

References

(1) Badgley, R. H. and Booker, J. G. 'Turborotor instability: effect of initial transient on plane motion', J. Lub. Tech., Trans. Amer. Soc. mech. Engrs. 1969, 625.

(2) Mitchell, J. R., Holmes, R., and Byrne, T. 'Oil whirl of a rigid rotor in 360° journal bearings: further characteristics', Proc. Inst. mech. Engrs. 1965 180 No. 25, 593.

(3) Castelli, V. and Elrod, H. G. 'Solution of the stability problem of 360 deg. self-acting gas-lubricated bearings', Trans. Amer. Soc. mech. Engrs., vol. 87, series D, No. 2, June, 1965, p. 199.

(4) Kirk, R. G. and Gunter, E. J. 'Transient journal bearing analysis', NASA CR-1549, 1970.

(5) Barrett, L. E. and Gunter, E. J. 'Steady-state and transient analysis of a squeeze film damper bearing for rotor stability', NASA CR-2548, May, 1975.

(6) Lund, J. W. 'Self-excited stationary whirl orbits of a journal in a sleeve bearing', Ph.D Thesis, 1966, Rennsselaer Polytechnic Inst., Troy, N. Y.

(7) Holmes, R. 'The vibration of a rigid shaft on short sleeve bearings', J. mech. Engng Sci. (Inst. mech. Engrs.) 1960 2 No. 4, 337.

(8) Kirk, R. G. and Gunter, E. J. 'Nonlinear transient analysis of multi-mass flexible rotors', NASA CR-2300, Sept. 1973.

(9) Falkenhagen, G. and Gunter, E. J. 'Nonlinear transient analysis of a rigid rotor supported by non-circular bearings', Research laboratories for the engineering sciences, University of Virginia, Charlottesville, Virginia, Report No. ME-4040-102-70U, 1970.

(10) Woodcock, J. S. and Holmes, R. 'The determination and application of the dynamic properties of a turbo-rotor bearing oil film', Proc. Inst. mech. Engrs. 184 Part 3L, 1969-70-72.

(11) Holmes, R. 'The effects of sleeve bearings on the vibration of rotating shafts', Tribology, August, 1972.

(12) Shawki, G. S. A. 'Whirling of a journal bearing experiment under no load condition', Engineering 179 1955, 92.

(13) Robertson, D. 'The whirling of shafts', Engineer, London 158 1934 216.

(14) Poritsky, H. 'Contribution to the theory of oil whip', Trans. ASME 75 1953 1153.

(15) Reddi, M. M. and Trumpler, P. R. 'Stability of the high-speed journal bearing under steady load', J. Engng Ing., Trans. Amer. Soc. mech. Engrs., vol. 84, series B, 1962, p. 351.

(16) Holmes, R. 'Oil whirl characteristics of a rigid rotor in 360° journal bearings', Proc. Inst. mech. Engrs. 177, No. 1 1963 291.

(17) Gunter, E. J., 'Dynamic stability of rotor-bearing systems', NASA-SP-113, 1966.

Table 1

Amplitudes and transmitted forces of limit cycles for various unbalance values, N = 10 500

Unbalance, EMU (dimensionless)	Phase Angle-Degrees (if orbit synchronous)	Amplitude (dimensionless)	Transmitted force (dimensionless)	Transmitted force (Actual Values) lb (N)
0.00	-----	0.75	----	----------
0.04	-----	0.73	5.49	171.9(764.6)
0.08	-----	0.71	3.41	213.5(949.6)
0.12	-----	0.67	2.43	228.0(1014.1)
0.16	-----	0.59	1.83	229.8(1022.1)
0.20	-----	0.45	1.35	212.1(943.4)
0.22	-----	0.44	1.25	214.6(954.5)
0.25	-----	0.30	1.03	202.4(900.3)
0.26	123.5	0.29	1.02	207.0(920.7)
0.27	125.0	0.30	1.03	217.7(968.3)
0.30	125.0	0.33	1.06	248.6(1105.8)
0.35	124.5	0.38	1.17	321.5(1430.0)
0.50	122.5	0.51	1.21	378.9(1685.3)
0.45	104.0	0.54	1.55	546.9(2432.6)
0.50	94.5	0.58	1.65	646.7(2876.5)
0.55	87.5	0.60	1.70	730.3(3248.4)
0.60	80.5	0.62	1.71	803.7(3574.9)
0.80	67.0	0.67	1.66	1041.3(4631.7)
2.50	39.5	0.78	1.31	2556.7(11372.2)

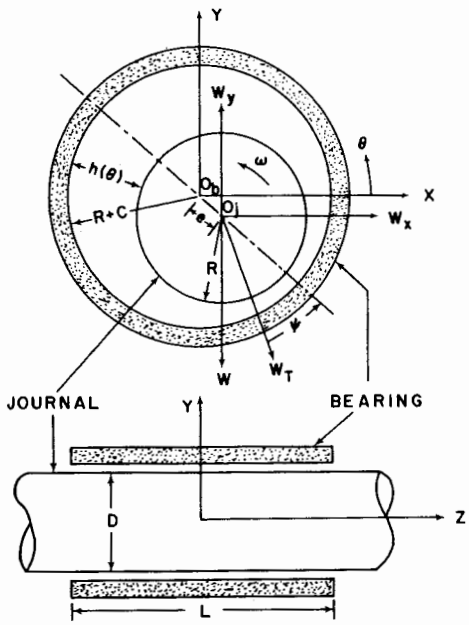

Fig. 1: Journal bearing schematic and coordinate system

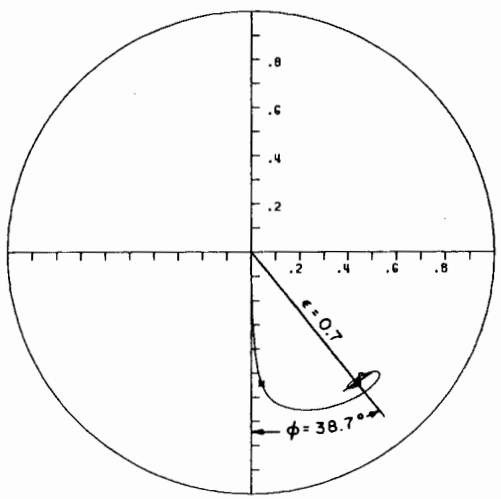

Fig. 2: Transient motion of a gravitationally loaded, balanced journal seeking equilibrium position. N = 2318 rev/min L/D = 0.333, C/R = 0.0048, W = 178 N, S = 0.305

This paper is prsented for written discussion. The MS was received on 14th August 1975 and accepted for publication on 16th March 1976. 32

Communications are invited for publication in the Proceedings. Contributors should read the instructions on page ii of cover.

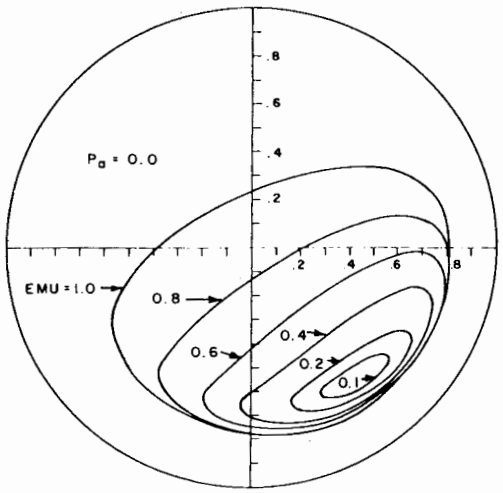

Fig. 3: Steady state synchronous whirl orbits about the equilibrium position for various values of dimensionless unbalance, N = 2416 rev/min, L/D = 0.333, C/R = 0.0048, W = 178 N, S = 0.305

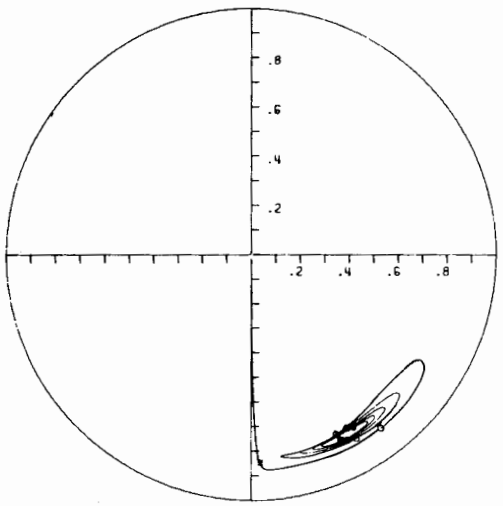

(a)

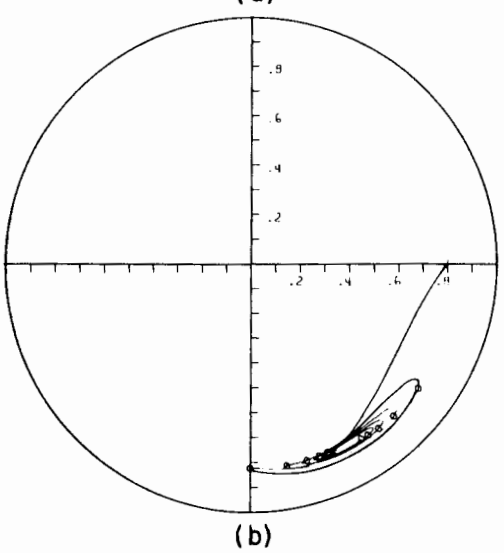

(b)

Fig. 4: Transient motion of a horizontal, balanced journal with different initial positions. (a) Motion started at origin with zero velocity, (b) Motion started at $\epsilon = 0.8$, $\phi = 90\%$ with zero velocity. N = 5700 rev/min, L/D = 0.62, C/R = 0.0147, W = 35.6 N, S = 0.02624, L = 11.8 mm, Pa = 0

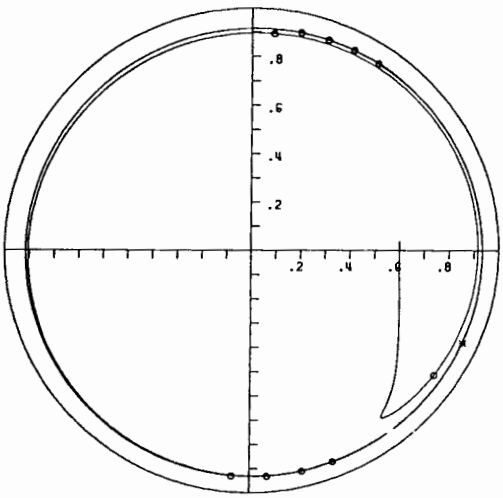

Fig. 5: Transient motion of a horizontal, balanced journal with high ambient pressure (p_a = 3.41 MPa). N = 5700 rev/min, L/D = 0.62, C/R = 0.0147, W = 35.6 N, S = 0.0262, L = 11.8

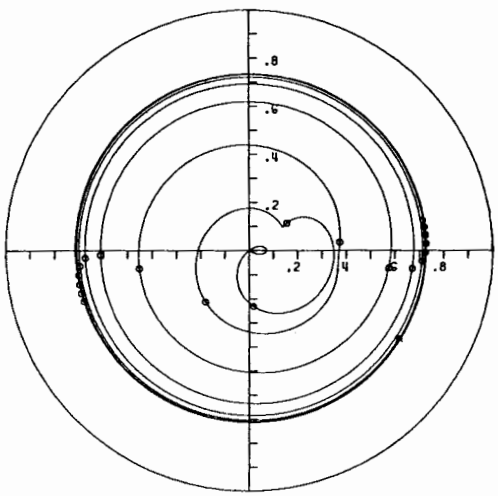

Fig. 6: Transient motion of slightly unbalanced journal operating above stability threshold speed (EMU = 0.08), N = 10500 rev/min, L/D = 0.5, C/R = 0.005, W = 222 N, S = 2.8, L = 24.5 mm, Pa = 0

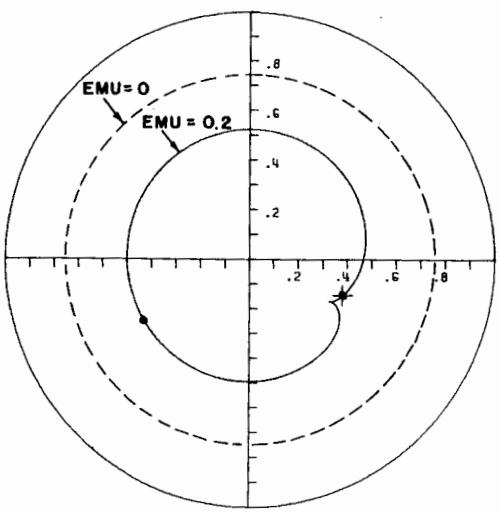

Fig. 7: Comparison of journal bearing limit cycle motion of a balanced and unbalanced journal (EMU = 0.2). N = 10500 rev/min, L/D = 0.5, C/R = 0.005, W = 222 N, S = 2.8, L = 25.4 mm, Pa = 0

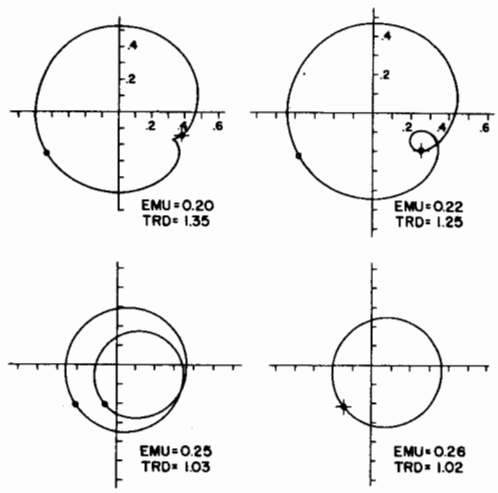

Fig. 8: Limit cycle motion and dynamic transmissibility for various values of unbalance for a journal operating above the stability threshold speed. N = 10500 rev/min, L/D = 0.5, C/R = 0.005, W = 222 N, S = 2.8, L = 25.4 mm, Pa = 0

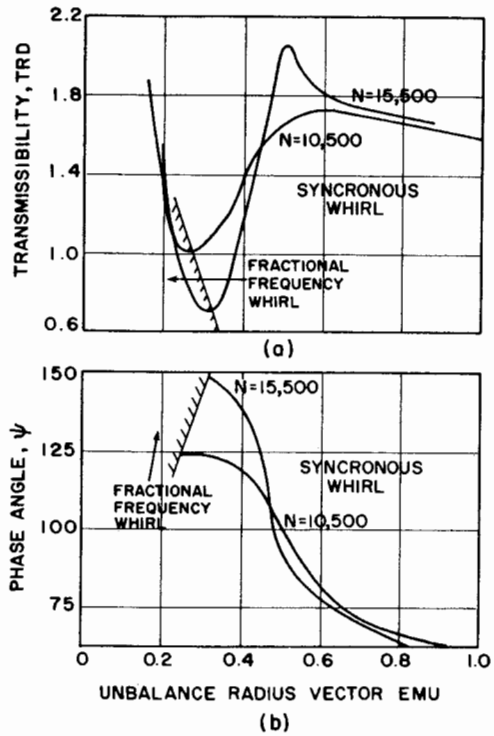

Fig. 9: Force transmissibility coefficient, TRD, and phase angle as functions of unbalance magnitude, EMU for journals operating above the stability threshold speed, N = 10500 and 15000 rev/min

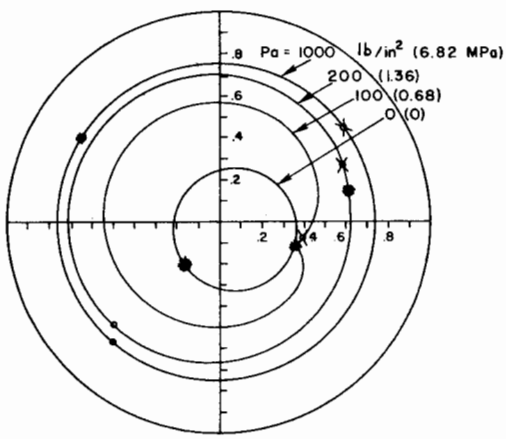

Fig. 10: Limit cycles of an unbalanced rotor (EMU = 0.26) for various levels of ambient pressure, N = 10500 rev/min, L/D = 0.5, C/R = 0.005, W = 222 N, S = 2.8, L = 25.4 mm